Spatial Power Combining for Two-Dimensional Structures

Chris W. Hicks, *Student Member, IEEE,* Huan-Sheng Hwang, *Member, IEEE,* Michael B. Steer, *Senior Member, IEEE,* James W. Mink, *Fellow, IEEE,* and James F. Harvey, *Member, IEEE*

***Abstract*— The two-dimensional (2-D) hybrid dielectric slab–beam open and closed waveguide systems are suitable for the design of planar quasi-optical integrated circuits and devices. An open system consisting of an active E-plane amplifier array consisting of Vivaldi-type antennas with MESFET and monolithic microwave integrated circuit (MMIC) devices was investigated. The 4 × 1 MESFET amplifier array generated 11 and 4.5 dB of amplifier and system gain, respectively, at 7.12 GHz, and the cascade MMIC Vivaldi-type antenna produced 24 dB of amplifier gain at 8.4 GHz. Also, experiments on a new 2-D H-plane parallel-plate closed system with a stripline slot antenna is introduced, and the wavebeam-mode theory is presented. The new system minimizes scattering and isolation losses associated with open structures. The amplifier gain of the closed system based on slot antennas is compared to the open system based on Vivaldi antennas.**

***Index Terms*—Power combining.**

I. Introduction

SPATIAL power combining has emerged as a promising technique for power combining at millimeter and submillimeter-wave frequencies. One embodiment of spatial power combining is quasi-optical power combining, in which radiation by individual elements of an array of solid-state active devices is combined utilizing wavebeam principles. Optical lenses are utilized to provide periodic refocusing of the beam and to combine power in a single paraxial mode. The large transverse and longitudinal dimensions of the quasi-optical structures provide a significant area for the active monolithic microwave integrated circuit (MMIC) devices and control components to be included within the structure. The most mature quasi-optical structures include grid amplifiers and resonant cavities where the power is combined in three-dimensional (3-D) space [1], [2]. However, two-dimensional (2-D) technology offers an alternative approach with significant advantages. Mink and Schwering [5] proposed a 2-D hybrid dielectric slab–beam waveguide (HDSBW) which is more amenable to photolithographic definition and fabrication, and is more compatible with MMIC technology [3], [4]. The 2-D HDSBW has reduced size and weight, and improved heat-removal capability, which results in lower costs.

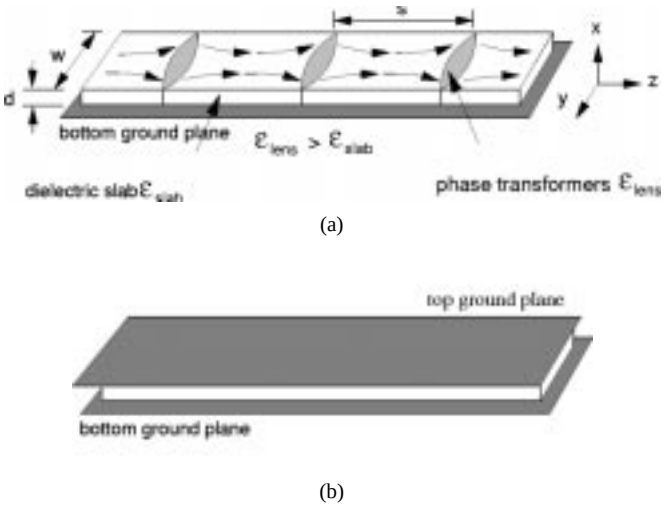

Fig. 1. Passive 2-D quasi-optical power combining system with concave lenses. (a) Open structure. (b) Closed structure.

The 2-D quasi-optical systems we have reported on are open planar structures, which consist of one ground plane and dielectric slab [see Fig. 1(a)]. Open systems have demonstrated the ability to combine power from a source array. In this paper, we document the lessons learned with the open structure, particularly excessive scattering losses. Here, we report on our work to minimize these losses using a closed 2-D slab–beam waveguide configuration, as show in Fig. 1(b). Beam-mode theory and experimental characterization of this configuration are presented.

II. Principles of Operation

Most recent work has demonstrated a viable 2-D quasi-optical power-combining system with an active E-plane amplifier array consisting of Vivaldi-type antennas using MESFET and MMIC devices, and convex and concave lenses. A 4 × 1 amplifier array generated 11 and 4.5 dB of amplifier and system gain, respectively, at 7.12 GHz, and the single MMIC Vivaldi-type antenna produced 24 dB of amplifier gain at 8.4 GHz (see Fig. 2). This system was tested with the array

Manuscript received November 6, 1997; revised march 4, 1998. This work was supported by the U.S. Army Research Office through Clemson University as a Multidisciplinary Research Initiative on Quasi-Optics under Agreement DAAG55-97-K-0132, and also by the Naval Air Warfare Center Aircraft Division, Code 4.5.5.5., RF Sensor Branch.

C. W. Hicks is with the Center for Advanced Computing and Communications, Department of Electrical and Computer Engineering, North Carolina State University, Raleigh, NC 27695-7914 USA, and with the Naval Air Warfare Center Aircraft Division, Code 4.5.5.5, Patuxent River, MD 27670-5304 USA.

H.-S. Hwang was with the Department of Electrical and Computer Engineering, North Carolina State University, Raleigh, NC 27695-7914 USA. He is now with Raychem Corporation, Fuquay-Varina, NC 27526 USA.

M. B. Steer and J. W. Mink are with the Center for Advanced Computing and Communications, Department of Electrical and Computer Engineering, North Carolina State University, Raleigh, NC 27695-7914 USA.

J. F. Harvey is with the Electronics Division, U.S. Army Research Office, Research Triangle Park, NC 27709-2211 USA.

Publisher Item Identifier S 0018-9480(98)04041-1.

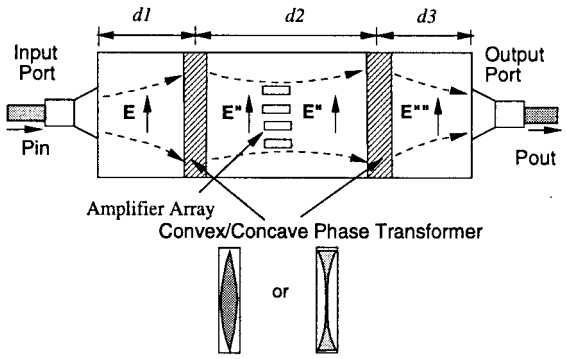

Fig. 2. The 2-D HDSBW system with convex/concave lenses and 4 × 1 MESFET amplifier array.

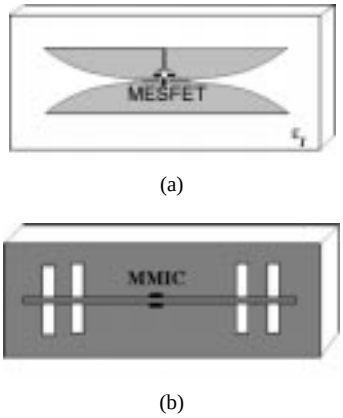

Fig. 3. Input and output coupling antennas on RT/Duriod substrate. (a) MESFET Vivaldi amplifier. (b) MMIC stripline slot amplifier.

placed on top of the dielectric slab and with the array located under the dielectric slab in the bottom ground plane. The transverse electric (TE) modal field solution shows that the electric-field distribution is high at the air-to-dielectric interface and reaches a minimum at the dielectric-to-ground interface. With the antenna located at the top interface, the high field distribution causes perturbations and variations, which make it difficult to predict and control the phase distribution of the array. Additional problems with the open structure consists of radiation losses from the dielectric top and sidewalls, beam confinement to within the dielectric slab, and scattering loss of the Vivaldi antenna [see Fig. 3(a)]. The losses associated with the open system can be minimized by using a closed system [see Fig. 1(b)], by placing the amplifier array under the dielectric slab in the ground plane, and utilizing a stripline slot antenna.

This paper extensively documents the Vivaldi antenna-based system and presents mode theory for the closed system and initial results for the preferred closed system with stripline slot-coupled antennas. A closed system employing two ground planes, a parallel-plate system, is used to minimize the losses associated with the open systems. The waveguide confines the transverse magnetic (TM) modal wavebeam, which provides maximum coupling to the source array located in the bottom ground plane. The system performance is also enhanced by replacing the Vivaldi antenna with a stripline slot antenna. The Vivaldi has greater bandwidth than the slot antenna; however, the Vivaldi has a larger metallic surface area that produces scatter. Also, the Vivaldi has poor isolation between the input and output antennas because the antennas and amplifier are on the same plane and the input and output are in close proximity. The stripline slot antenna can be used in a multilayer configuration, with the slots and amplifier located in different planes, thereby improving isolation between the input and output slots, and minimizing scattering loss.

Both open and closed HDSBW systems utilize two distinct waveguiding principles to guide the electromagnetic wave [5], [7]. For the open system, the field distribution in the x-direction is that of a surface-wave mode of the grounded dielectric slab; the wave is guided by total reflection at the air-to-dielectric interface, and parameters are adjusted such that energy is transmitted primarily within the dielectric. In the closed system, the field distribution in the x-direction is that of a parallel-plate waveguide. In both systems, the field

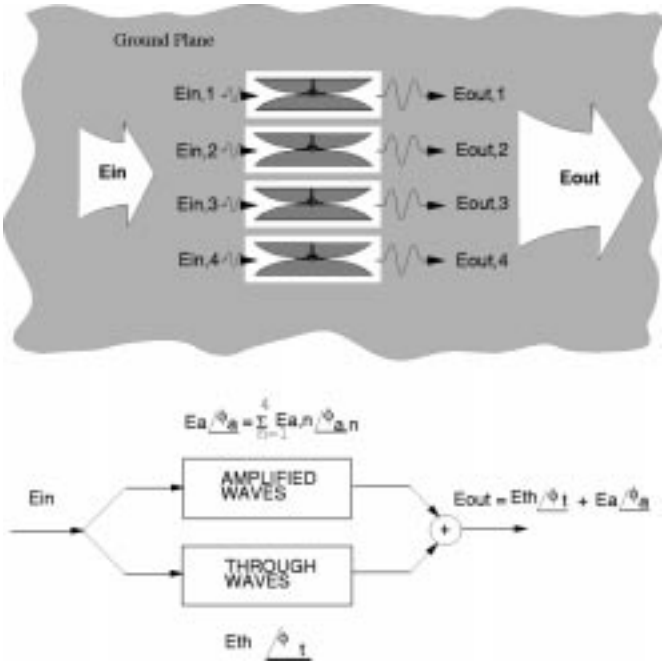

Fig. 4. Electric-field wave model for 2-D power-combining system.

distribution in the y-direction is that of a wavebeam mode (Guass–Hermite), which is guided by the lenses through periodic reconstitution of the cross-sectional phase distribution. The guided modes are either TE or TM polarized with respect to the direction of propagation. The theory for the 2-D open HDSBW was developed by Mink and Schwering [4].

The 2-D HDSBW principle is used to obtain signal amplification similar to that of a traveling-wave amplifier. An array of active elements located underneath the dielectric slab is placed in the path of the wavebeam, as shown in Fig. 4. Each active element consists of a pair of back-to-back Vivaldi or slot antennas with an amplifier or MMIC inserted between the two antennas. Part of the incident signal, the through wave, passes through the dielectric slab undisturbed.

The remaining signal is amplified by the array. The first Vivaldi or slot antenna couples energy from the incident traveling wavebeam, and the second antenna reinserts the amplified signal back into the traveling wavebeam. Maximum coupling to the array occurs when the energy from the first lens focuses

energy to the input of the antennas. The signal is amplified by the MESFET's and is coupled by the output antennas to the traveling wavebeam, where it combines in phase with the through signal. Consequently, a growing traveling wavebeam mode is established within the guiding structure resulting in increased output power.

III. Beam-Mode Theory in a Closed Slab–Beam Waveguide

The closed 2-D power-combining systems consist of two parallel conducting planes separated by a dielectric slab with relative permittivity ϵ_r of thickness d. The fields in the waveguide are found from Helmholtz equations and the proper boundary conditions. This leads to solutions for the scalar axial fields in the waveguide. Once the axial components are found, the transverse fields are derived from Maxwell's equations. By applying orthogonality conditions, the fields are normalized and the normalized power in the parallel-plate waveguide can be computed. The general solution of the transverse and longitudinal fields for the guiding structure is obtained from Helmholtz equations [8]

$$\nabla^2\mathbf{H}+k^2\mathbf{H}=0 \tag{1a}$$

$$\nabla^2\mathbf{E}+k^2\mathbf{E}=0. \tag{1b}$$

The fields in the waveguide are classified as TE and TM waves with transverse and axial components

$$\mathbf{H}^{\pm}_{\mathbf{mn}}=(\pm\mathbf{h}_{\mathbf{mn}}+h_{\mathrm{zmn}}\hat{a}_z)e^{\mp\beta_{mn}z} \tag{2a}$$

$$\mathbf{E}^{\pm}_{\mathbf{mn}}=(\mathbf{h}_{\mathbf{mn}}\pm e_{\mathrm{zmn}}\hat{a}_z)e^{\mp\beta_{mn}z} \tag{2b}$$

where $\mathbf{e}_{\mathbf{mn}}$ and $\mathbf{h}_{\mathbf{mn}}$ are transverse vector functions, while e_{zmn} and h_{zmn} are axial scalar functions. The term β_{mn} is the propagation constant and m and n are the mode indexes for the x- and y-directions, respectively. The TE-mode solution is obtained when $h_{\mathrm{zmn}}=0$, while the TM-mode solution is obtained when $e_{\mathrm{zmn}}=0$. All the transverse fields can be expressed in terms of the axial components. Substituting (2) into (1) results in TE modes with

$$h_{mn}=-\frac{j\beta_{mn}}{k_c^2}\nabla_t h_{\mathrm{zmn}}e^{\mp\beta_{mn}z} \tag{3a}$$

$$e_{mn}=Z_h\hat{a}_z\times h_{mn} \tag{3b}$$

and TM modes with

$$e_{mn}=-\frac{j\beta_{mn}}{k_c^2}\nabla_t e_{\mathrm{zmn}}e^{\mp\beta_{mn}z} \tag{4a}$$

$$h_{mn}=Y_e\hat{a}_z\times e_{mn} \tag{4b}$$

where $Y_e=jk_0Y_0/\beta_{mn}$ is the scalar-wave admittance and $Z_h=jk_0Z_0/\beta_{mn}$ is the scalar-wave impedance where $Z_0=(1/Y_0)$ and Y_0 are the intrinsic impedance and admittance of free space. The boundary conditions for the parallel-plate mode structures are

$$\text{TM}\qquad e_{\mathrm{zmn}}=0 \text{ at } x=0 \text{ and } x=d \tag{5a}$$

$$\text{TE}\qquad \partial h_{\mathrm{zmn}}/\partial y=0 \text{ at } y=-\infty \text{ and } y=+\infty. \tag{5b}$$

Through separation of variables, the axial components for the parallel-plate guiding structure take the following form:

$$\text{TM}\qquad e_{\mathrm{zmn}}=A_{mn}X_m(x)Q_n(y,z) \tag{6a}$$

$$\text{TE}\qquad h_{\mathrm{zmn}}=B_{mn}X_m(x)Q_n(y,z) \tag{6b}$$

where A_{mn} and B_{mn} are the electric- and magnetic-field normalization factors, respectively, which are yet to be determined. Utilizing the boundary conditions (5), the $X_m(x)$ function is expressed in terms of orthogonal sine and cosine functions in the x-direction for e_{zmn} and h_{zmn}, while the $Q_n(z,y)$ function describes the slow variation in the y-direction. It is defined as [1]

$$\begin{aligned}Q_n(y,z)=&\frac{1}{\sqrt{Yn!\sqrt{\pi}}}(1+\nu_{mn}^2)^{1/4}\\&\cdot He_n\left(\frac{\sqrt{2}y}{y_{\mathrm{zmn}}}\right)\cdot\exp\left[-\left(\frac{y}{y_{\mathrm{zmn}}}\right)^2\right]\\&\pm\exp j\left[\nu_{mn}\left(\frac{y}{y_{\mathrm{zmn}}}\right)^2-\left(n+\tfrac{1}{2}\right)\tan^{-1}(\nu_{mn})\right]\end{aligned} \tag{7}$$

where

$$\nu_{mn}=\frac{z}{\beta_m n}\overline{Y}^2\quad y_{\mathrm{zmn}}=\overline{Y}^2(1+\nu_{mn}^2)$$

and

$$\overline{Y}^2=\left[\frac{\sqrt{(2-D/F)FD}}{\beta_{mn}}\right]^{1/2}$$

where D is the distance between the reflecting surfaces, and F is the focal length of the lenses. The term Q_n is composed of Hermite polynomials, which is a complete set of orthogonal functions. Similarly, Q_n also forms a complete set of orthonormal functions. By substituting the axial equations into the scalar-wave equations, it is found that the propagation constant β_{mn} is restricted as $\beta_{mn}^2=k_0^2-k_c^2$ where $k_0^2=\omega^2\mu_0\epsilon_0$, $k_x^2=m\pi/d$, and $k_y^2=-[\partial^2Q_n(y,z)/\partial y^2]/Q_n(y,z)$. By substituting the axial fields (6) into (3) and (4), the transverse fields for the TM mode are

$$e_{\mathrm{zmn}}=A_{mn}\sin\left(\frac{m\pi x}{d}\right)Q_n(y,z) \tag{8a}$$

$$e_{xmn}=-A_{mn}\left(\frac{j\beta}{k_c}\right)\left(\frac{m\pi}{d}\right)\cos\left(\frac{m\pi x}{d}\right)Q_n(y,z) \tag{8b}$$

$$e_{ymn}=-A_{mn}\left(\frac{j\beta}{k_c}\right)\sin\left(\frac{m\pi x}{d}\right)\frac{\partial Q_n(y,z)}{\partial y} \tag{8c}$$

and the magnetic fields are

$$h_{xmn}=Y_e e_{ymn} \tag{8d}$$

$$h_{ymn}=-Y_e e_{xmn}. \tag{8e}$$

The fields for the TE case are

$$h_{\mathrm{zmn}}=B_{mn}\cos\left(\frac{m\pi x}{d}\right)Q_n(y,z) \tag{9a}$$

$$h_{xmn}=-B_{mn}\left(\frac{j\beta}{k_c}\right)\left(\frac{m\pi}{d}\right)\sin\left(\frac{m\pi x}{d}\right)Q_n(y,z) \tag{9b}$$

$$h_{ymn}=-B_{mn}\left(\frac{j\beta}{k_c}\right)\cos\left(\frac{m\pi x}{d}\right)\frac{\partial Q_n(y,z)}{\partial y} \tag{9c}$$

and the electric fields are

$$e_{xmn}=Z_h h_{ymn} \tag{9d}$$

$$e_{ymn}=-Z_h h_{xmn} \tag{9e}$$

where (8) and (9) represent the transverse fields in the parallel-plate HDSBW.

A. Orthogonality of Fields

After the fields for the parallel-plate waveguide have been determined, the fields can be normalized to satisfy the orthogonality relationship. The TM and TE orthogonality relationships, respectively, are given as

$$\int_0^d \int_{-\infty}^{\infty} e_{mn} \cdot e^*_{m'n'}\, dx\, dy = \delta'_{mm}\delta'_{nn} \tag{10a}$$

$$\int_0^d \int_{-\infty}^{\infty} h_{mn} \cdot h^*_{m'n'}\, dx\, dy = \delta'_{mm}\delta'_{nn}. \tag{10b}$$

The normalization factor needed to satisfy the TE and TM orthogonality relations are obtained from the orthogonal equation (11a)–(11c), shown at the bottom of the page. Now, the transverse fields (8) and (9), and the orthogonal equation (11a)–(11c) are substituted into (10). The result becomes

$$\int_0^d \int_{-\infty}^{\infty} e_{mn} \cdot e^*_{m'n'}\, dx\, dy = \int_0^d \int_{-\infty}^{\infty} h_{mn} \cdot h^*_{m'n'}\, dx\, dy = D_{mn}\delta_{mm'}\delta_{nn'} \tag{12}$$

where D_{mn} is a constant, which is defined as

$$D_{mn} = \left(\frac{\beta_m}{k_c^2}^2\right)\frac{d}{2}\left\{\frac{m\pi}{d} + n + \frac{(n+1/2)}{y_{\text{zmn}}^2 + \dfrac{v_{mn}}{y_{\text{zmn}}^4}}\right\}. \tag{13}$$

Now, this constant is used to determine the electric and magnetic normalization factors. From (12), it is seen that the normalization factors are equal when they are redefined as $A_{mn} = B_{mn} = 1/\sqrt{D_{mn}}$. By using this relation, the transverse fields will be normalized and the TM and TE orthogonality relations (10) will be satisfied. From here, it will be assumed that all the transverse fields are normalized. The mnth-mode electric and magnetic fields propagating in the $+z$-direction are represented as

$$\mathbf{E}^+_{\mathbf{mn}} = (\mathbf{e_{mn}} + \mathbf{e}_{\text{zmn}})e^{-\beta_{mn}z} \tag{14a}$$

$$\mathbf{H}^+_{\mathbf{mn}} = (\mathbf{h_{mn}} + \mathbf{h}_{\text{zmn}})e^{-\beta_{mn}z} \tag{14b}$$

the mnth-mode fields propagating in the $-z$-direction are given as

$$\mathbf{E}^-_{\mathbf{mn}} = (\mathbf{e_{mn}} - \mathbf{e}_{\text{zmn}})e^{\beta_{mn}z} \tag{15a}$$

$$\mathbf{H}^-_{\mathbf{mn}} = (-\mathbf{h_{mn}} + \mathbf{h}_{\text{zmn}})e^{\beta_{mn}z} \tag{15b}$$

where $\mathbf{E}^+_{\mathbf{mn}}$, $\mathbf{H}^+_{\mathbf{mn}}$, and $\mathbf{E}^-_{\mathbf{mn}}$, $\mathbf{H}^-_{\mathbf{mn}}$ are the forward and backward traveling electric and magnetic fields, respectively. The total electric and magnetic fields propagating in the $+z$-direction are then expressed as

$$\mathbf{E}^+ = \sum_{mn} a_{mn}\mathbf{E}^+_{\mathbf{mn}} \tag{16a}$$

$$\mathbf{H}^+ = \sum_{mn} a_{mn}\mathbf{H}^+_{\mathbf{mn}} \tag{16b}$$

and in the $-z$-direction, the total fields are

$$\mathbf{E}^- = \sum_{mn} b_{mn}\mathbf{E}^-_{\mathbf{mn}} \tag{17a}$$

$$\mathbf{H}^- = \sum_{mn} b_{mn}\mathbf{H}^-_{\mathbf{mn}} \tag{17b}$$

where a_{mn} and b_{mn} are expansion coefficients which can be determined from the excitation fields and the Lorentz reciprocity theorem.

B. Power Normalization

Mode orthogonality between the fields means that each mode is independent of the other modes, it carries its own power, and there is no power coupled between modes. The general expression for the power propagating inside a waveguide in the $+z$-direction is

$$P_{mn} = \tfrac{1}{2}\,\text{Re}\int_0^d \int_{-\infty}^{\infty} \mathbf{E}^+ \times \mathbf{H}^{+^*} \cdot \hat{a}_z\, dx\, dy. \tag{18}$$

Since the fields are orthogonal, the normalized power in the waveguide can be found from the TM and TE orthogonal relationships (10). The normalized power propagating in the $+z$-direction is found to be

$$p_{mn} = a_{mn}a^*_{m'n'}\delta_{mm'}\delta_{nn'} \tag{19}$$

where $p_{mn} = 2P_{mn}Y_e$ for the TE modes and $p_{mn} = 2P_{mn}/Z_h$ for the TM modes.

C. Verification

The theory of the closed system was verified by testing a confocal parallel-plate cavity system. The geometry for the parallel-plate resonator is shown in Fig. 5. The width and length are denoted by $a = 30.48$ cm and $b = 30$ cm, the radius of curvature is denoted by $r = 60.96$ cm. The upper and lower ground planes are separated by a dielectric (Rexolite $\epsilon_r = 2.57$) with thickness $d = 1.27$ cm. An L-shaped coaxial probe normal to the ground plane was used to excite the cavity. The resonate frequencies for the parallel-plate cavity

---

$$\int_0^d \cos\frac{m\pi x}{d} \cdot \cos\frac{m'\pi x}{d}\, dx = \begin{cases} \dfrac{d}{2}\,\delta_{mm'}, & m = m' \\ 0, & m \neq m' \end{cases} \tag{11a}$$

$$\int_0^d \sin\frac{m\pi x}{d} \cdot \sin\frac{m'\pi x}{d}\, dx = \begin{cases} \dfrac{d}{2}\,\delta_{mm'}, & m = m' \\ 0, & m \neq m' \end{cases} \tag{11b}$$

$$\int_{-\infty}^{\infty} \left[\frac{\partial Q_n(y,z)}{\partial y}\right]\left[\frac{\partial Q_{n'}(y,z)}{\partial y}\right] dy = \begin{cases} n + \dfrac{n+1/2}{y_{\text{zmn}}^2} + \dfrac{\nu_{mn}}{y_{\text{zmn}}^4}\,\delta_{nn'}, & n = n' \\ 0, & n \neq n' \end{cases} \tag{11c}$$

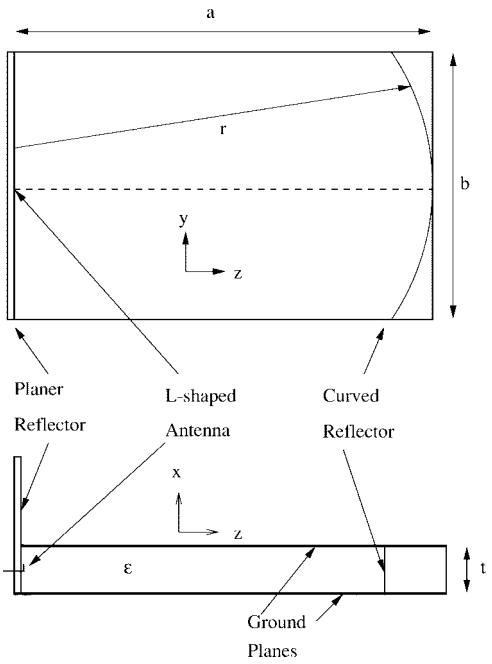

Fig. 5. Test configuration for the confocal parallel-plate resonator system.

are calculated from

$$\beta_m z - (n+\tfrac{1}{2})\tan^{-1}\nu_{mn} = q\pi. \tag{20}$$

Solving the above equation for the resonance frequencies of the parallel-plate cavity structure gives

$$f_{mn} = \frac{c}{2\pi\sqrt{\epsilon_r}} \cdot \left\{ \frac{q\pi + (n+\frac{1}{2})\tan\left[z/\sqrt{(2-D/F)FD}\right]^2}{z} + \left(\frac{m\pi}{d}\right)^2 \right\}^{1/2} \tag{21}$$

where m, n, and q are the mode indexes for the x-, y-, and z-directions, respectively. Measurements were obtained by using a Hewlett-Packard 8510C Vector Network Analyzer to measure S_{11} of the resonator. An L-shaped coaxial probe normal to the ground plane was used to excited the TM modes inside the cavity. The $\mathrm{TM}_{0,m,q}$ modes was selected because $m = 0$ signifies the dominate mode inside a parallel-plate waveguide. Fig. 6 shows S_{11} versus resonant frequencies. A 1/2-in dielectric slab has a cutoff frequency of 7.367 GHz for the $\mathrm{TM}_{1,0,0}$ mode, which was predicted and measured. Above the cutoff frequency, high order modes appeared. The plot shows that the signal increases as frequency increases and peaks at 6.869 GHz, which is identified as the $\mathrm{TM}_{0,0,22}$ mode. This mode and other frequencies have also been predicted. The theory was also used to predict the frequency spacing $b = 307$ MHz between two adjacent TM modes.

D. Mode Profile

The profile of the electric-field distribution was measured by inserting a small vertical coaxial probe in the top ground plane 15 cm from the planar reflector in the z-direction. Measurements were conducted at 6.898 GHz ($\mathrm{TM}_{0,1,22}$ resonant frequency) by sliding the probe in the y-direction in 5-mm

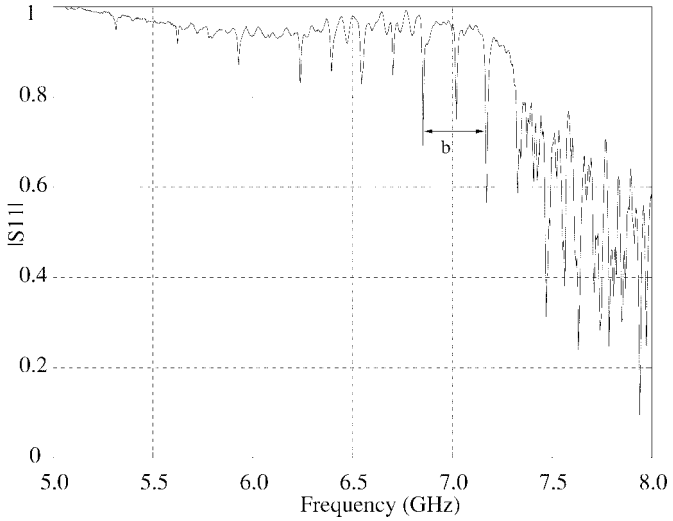

Fig. 6. Resonant frequencies for a confocal 2-D parallel-plate resonator system.

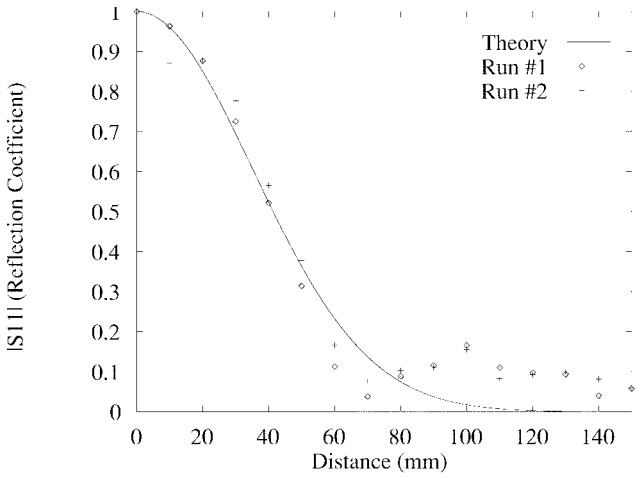

Fig. 7. Electric-field mode profile at 6.898 GHz for the parallel-plate confocal system.

TABLE I
SELECTED RESONATE FREQUENCIES OF THE PARALLEL-PLATE CAVITY SYSTEM

Measured Frequency (GHz)	Calculated Frequency (GHz)	Error (GHz)	n	q
6.869	6.868	0	1	22
6.719	6.715	0.004	3	21
6.558	6.561	0.003	1	21
6.408	6.408	0	3	20
6.254	6.254	0	1	20

increments. Two sets of measurements or runs were performed. The plot of the measured data and the ideal data, shown in Fig. 7 and Table I, indicate that the theory and measurements show good agreement.

Errors of the system are due to the finite length of the vertical probe, which resulted in small errors due to the estimation of the focal length, metallic losses of the upper and lower ground planes, and reflector, dielectric losses, and leakage from the sidewalls of the resonator. In order to minimize reflections from the sides of the dielectric, the dielectric was tapered at the edges. The total error associated with this measurement is 5%–10%.

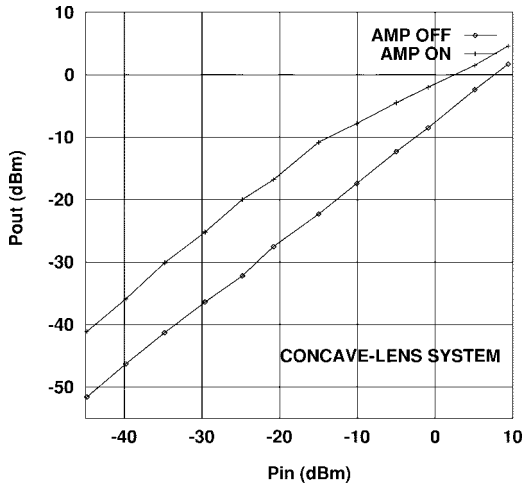

Fig. 8. Input and output power of the concave-lens 4 × 1 MESFET array.

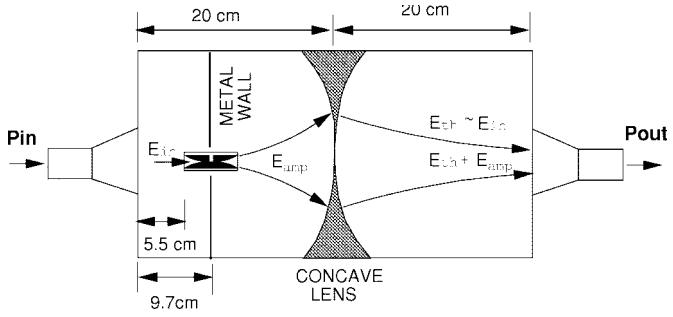

Fig. 9. The concave-lens system configuration for a unit-cell amplifier.

IV. Experimental Results

A. Open System Configuration

The system configuration for the open TE HDSBW, shown in Fig. 2, consists of a rectangular dielectric slab made of Rexolite ($r = 2.57$, $\tan\delta = 0.0006$) placed on a conducting ground plane. Two concave cylindrical lenses made of Macor ($r = 5.9$, $\tan\delta = 0.0006$) with focal lengths equal to 28.54 cm were inserted into the dielectric slab. The dielectric slab dimensions length ($d1+d2+d3$), width (w), and thickness (d) were 62, 27.94, and 1.27 cm, respectively. The Vivaldi antenna MESFET amplifiers were located underneath the dielectric slab in the ground plane. Each Vivaldi antenna was fabricated using RT/Duroid 6010 as the substrate ($\epsilon_r = 10.2$, $\tan\delta = 0.0028$) with the dimensions 6.5 cm × 1.5 cm. Two E-plane horns were designed and fabricated to efficiently launch and receive the required wavebeam. Two tests were performed on the open system, the first utilized a 4 × 1 MESFET Vivaldi amplifier array and the second employed a single MMIC Vivaldi amplifier located under the dielectric slab. A measure of the relative energy coupled to the amplifier array was obtained by switching the amplifier bias levels off and on while measuring the output power P_{out}. The system performance for the active Vivaldi amplifier array was determined by the system and amplifier gains. This provided an indication of the incident signal that passes through the dielectric as an undisturbed traveling wave.

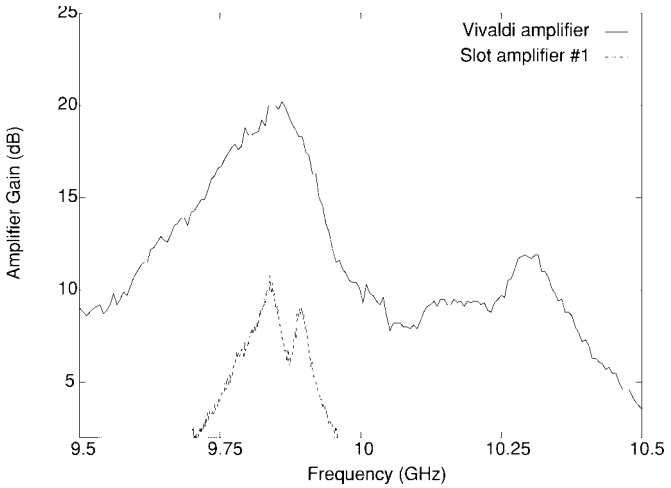

Fig. 10. Amplifier gain for a unit-cell amplifier with MMIC chips. (a) Vivaldi cascade MMIC's. (b) Slot single MMIC.

Fig. 8 shows the total system performance of the TE MESFET amplifier array at 7.12 GHz using concave lenses. A plot of P_{in} versus P_{out} is indicated by AMP OFF and AMP ON, respectively. The input power P_{in} varied from −45 dBm to +10 dBm in +5-dBm increments. The power ratio between P_{out} and P_{in} was relatively constant for P_{in} less than −15 dBm; however, P_{out} reached the saturation condition with P_{in} greater than −15 dBm. The maximum system gain of 4.5 dB occurred at $P_{\text{in}} = -15$ dBm, while the amplifier gain on to off measured was 11 dB.

B. Vivaldi Unit Cell

The second open TE system test was performed with a cascaded pair of MMIC amplifiers in order to achieve higher power levels. In Fig. 9, the amplifier gain of the Vivaldi amplifier was determined by placing a metal screen transverse to the Vivaldi structure. The Vivaldi amplifier and the metal wall were placed 5.5 and 9.7 cm, respectively, from the input horn. A concave lens was placed in the middle of a 40-cm dielectric slab. The slit in the metal wall allowed for only input power of the amplifier and the amplified energy to go through the system so that the amplifier gain could be measured. The amplifier gain was determined by switching the bias voltage on and off, while measuring the power difference detected by the receiving horn. The amplifier gain indicates that more than 20 dB of gain was produced from 7 to 10.5 GHz with a maximum gain of 24 dB at 8.4 GHz. The gain from 9.5 to 10.5 GHz is shown in Fig. 10.

C. Unit-Cell Slot Antenna

As a means of comparison, a TM unit-cell slot antenna was tested and compared to the TE Vivaldi unit-cell antenna. The slot antenna had only one MMIC during this test and the lens was not utilized. The TM unit cell was placed in a parallel-plate configuration and located in the bottom ground plane under a 1/8-in Rexolite dielectric slab. In a similar manner, a metal wall was placed 8 mm from the middle of the input and output slot antenna where the MMIC was located. Two H-plane horns were designed to transmit and receive power, and to vertically polarize the electric field so that maximum

coupling occurs in the slots. The slots were located $\lambda/4$ apart and the slot width and length were $\lambda/10$ and $\lambda/2$, respectively.

Fig. 10 compares the unit cell Vivaldi and slot amplifier gain. The nominal gain of the MMIC at 10 GHz is 10 dB. Different gains were achieved because the Vivaldi was used in a cascade configuration, while the slot used only one MMIC. Another difference is that the Vivaldi was tested over a wider range than the slot. The Vivaldi reached 20 dB of gain, whereas the gain of the slot antenna with one MMIC reached 10 dB.

V. Conclusions

A 2-D HDSBW spatial power-combining system suitable for planar integrated circuits and devices has been presented. A system using concave lenses and TE Vivaldi-type antennas with MESFET and MMIC devices has been demonstrated. The system with a Vivaldi antenna-based unit cell was shown to have reasonable gain, but to have excessive scattering loss. Initial results for a TM closed system with stripline coupled slots was presented as a refinement. The beam-mode theory for this new system was developed and verified.

References

[1] J. W. Mink, "Quasi-optical power combining of solid-state millimeter-wave sources," *IEEE Trans. Microwave Theory Tech.*, vol. MTT-34, pp. 273–279, Feb. 1986.

[2] Z. B. Popovic, R. M. Weilke, M. Kim, and D. B. Rutledge, "A 100-MESFET planar grid oscillator," *IEEE Trans. Microwave Theory Tech.*, vol. 39, pp. 193–200, Feb. 1991.

[3] H. Hwang, G. P. Monahan, M. B. Steer, J. W. Mink, J. Harvey, A. Paollela, and F. K. Schwering, "A dielectric slab waveguide with four planar power amplifiers," in *IEEE MTT-S Int. Microwave Symp. Dig.*, Orlando, FL, May 1995, pp. 921–924.

[4] A. R. Perkons and T. Itoh, "A 10-element active lens amplifier on a dielectric slab," in *IEEE MTT-S Int. Microwave Symp. Dig.*, San Francisco, CA, June 1996, pp. 119–122.

[5] J. W. Mink and F. K. Schwering, "A hybrid dielectric slab–beam waveguide for the millimeter wave region," *IEEE Trans. Microwave Theory Tech.*, vol. 41, pp. 1720–1729, Oct. 1993.

[6] F. Poegel, S. Irrgang, S. Zeisberg, A. Schuenemann, G. P. Monahan, H. Hwang, M. B. Steer, J. W. Mink, F. K. Schwering, A. Paollela, and J. Harvey, "Demonstration of an oscillating quasi-optical slab power combiner," in *IEEE MTT-S Int. Microwave Symp. Dig.*, Orlando, FL, May 1995, pp. 917–920.

[7] R. A. York and Z. B. Popovic, *Active and Quasi-Optical Arrays for Solid-State Power Combining.* New York: Wiley, 1997, pp. 277–292.

[8] R. E. Collin, *Field Theory of Guided Waves.* New York: IEEE Press, 1991.

Chris W. Hicks (S'95) received the B.S. degree in electrical engineering from the University of South Carolina, Columbia, in 1985, the M.S.E.E. degree from North Carolina A&T State University, Greensboro, in 1994, and is working toward the Ph.D. degree from North Carolina State University, Raleigh.

Since 1985, he has been with the Naval Air Warfare Center-Aircraft Division (NAWC-AD), Patuxent River, MD. In 1985, he worked in the Laboratory Instruments and Standards Section, where he researched and developed automated microwave measurement systems to support avionic radar support systems. In 1996, he joined the RF Sensors Branch, where he conducts research for microwave millimeter-wave applications. His interests are microwave theory and measurement techniques, microwave passive and active circuits, applied electromagnetics, and phased-array antennas.

Mr. Hicks was the recipient of a NAWC-AD Fellowship.

Huan-Sheng Hwang (S'94–M'98) received the B.S.E.E. degree from Tutung Institute of Technology, Taipei, Taiwan, R.O.C., in 1984, and the M.S.E.E. and Ph.D. degrees from North Carolina State University, Raleigh, in 1993 and 1997, respectively.

He is currently with Raychem Corporation, Fuquay-Varina, NC. He has coauthored a book chapter, "Dielectric Slab Combiners," in *Active and Quasi-Optical Arrays* (New York: Wiley, 1997). His research interests include quasi-optical and spatial power-combining system, antennas, electromagnetics, RF and microwave/millimeter-wave components and circuits, and optics.

Dr. Hwang received the Prestigious Bronze Medallion for Outstanding Scientific Achievement presented at the 20th U.S. Army Science Conference, which is the second highest award for research throughout the Army.

Michael Steer (S'76–M–'78–SM'90) received the B.E. and Ph.D. degrees in electrical engineering from the University of Queensland, Queens., Brisbane, Australia, in 1978 and 1983, respectively.

He is currently Director of the Electronics Research Laboratory and Professor of electrical and computer engineering at North Carolina State University, Raleigh. His expertise in teaching and research involves circuit-design methodology. From a teaching perspective, he has taught courses at the sophomore through advanced graduate level in circuit design, including basic circuit design, analog integrated-circuit design, RF and microwave circuit design, solid-state devices, and computer-aided circuit analysis. He teaches video-based courses on computer-aided circuit analysis and on RF and microwave-circuit design, which are broadcast nationally by the National Technological University. His research has been directed at developing RF and microwave design methodologies, with the majority of contributions to microwave and millimeter-wave circuit simulation technology. Until 1996, he was the Librarian of the industry-based IBIS Consortium, which provides a forum for developing behavioral models. A converter written by his group to automatically develop behavioral models from a SPICE netlist is being used by upwards of 100 companies and has been incorporated in several commercial computer-aided engineering programs. He has organized many workshops and taught many short courses on signal integrity, wireless, and RF design. He has authored or co-authored over 140 papers and book chapters on topics related to RF and microwave design methodology. His current interests in RF and microwave design are being applied to the computer-aided engineering of quasi-optical power combining systems, the implementation of a 2-D quasi-optical power combining system, high-efficiency low-cost RF technologies for wireless applications, and computer-aided engineering of mixed digital, analog, and microwave circuits, which is largely funded by the Department of Defense through DARPA and the U.S. Army Research Office. He has worked on projects sponsored by the National Science Foundation, the U.S. Army Research Office, SEMATECH, Airforce Office of Scientific Research, Kobe Steel, MCNC, Defense Advanced Research Projects Agency, BNR, DEC, IBM, Analog Devices, Compact Software, and Scientific Research Associates. The quasi-optical power combining systems will, for the first time, provide significant power at millimeter-wave frequencies, enabling a variety of military and commercial systems to be developed.

Dr. Steer is a member of the International Union of Radio Science (URSI) and Commission D. He is active in the IEEE Microwave Theory and Techniques Society (MTT-S). In 1997, he was secretary of the MTT-S and is an elected member of the MTT Administrative Committee for the 1998–2001 term. In the MTT-S, he also serves on the Technical Committees on Field Theory and on Computer Aided Design. He is a 1987 Presidential Young Investigator.

James W. Mink (S'59–M'65–SM'81–F'91) received the Ph.D. degree in electrical engineering from the University of Wisconsin at Madison, in 1964.

From 1976 to 1994, he was with the U.S. Army Research Office, cumulating his service as the Director of the Electronics Division. From 1964 to 1976, he was the Research Physical Scientist for the U.S. Army at Fort Monmouth, NJ. In addition, from 1979 to 1994, he served as the Principal U.S. Army Representative of the Joint Services Electronics Program. In 1994, he joined North Carolina State University, Raleigh, on a full-time basis, where he is currently a Visiting Professor in the Department of Electrical and Computer Engineering. He was associate editor of *Channel Characterization* (New York: IEEE Press, 1976). He has published or presented over 60 refereed papers and holds 5 patents. His research continues to focus upon millimeter-wave systems and devices and upon conformal antennas, in particular, as applied to wireless communications. Since 1987, he has served as a program evaluator for ABET.

Dr. Mink is a member of the IEEE Antennas and Propagation Society ADCom since 1996, and Best Paper Awards Committee since 1982. He has served as editor of the IEEE TRANSACTIONS ON MICROWAVE THEORY AND TECHNIQUES since 1997, and as an associate editor for IEEE TRANSACTIONS ON ANTENNAS AND PROPAGATION from 1983 to 1989. He was guest editor of the IEEE TRANSACTIONS ON MICROWAVE THEORY AND TECHNIQUES Special Issues on Quasi-Optical Techniques and Numerical Methods. He has served on the IEEE Centennial Medals Committee.

James F. Harvey (M'91) for a photograph and biography, see this issue, p. 726.